those manipulators, described in the previous sections, constituting the torso and the arms.

Alternatively, it is possible to consider intermediate transformation matrices between the relevant structures. In detail, as illustrated in Fig. 2.28, if t denotes the frame attached to the torso, r and l the base frames, respectively, of the right arm and the left arm, and rh and lh the frames attached to the two hands (end-effectors), it is possible to compute for the right arm and the left arm, respectively:

$$\boldsymbol{T}_{rh}^{0} = \boldsymbol{T}_{3}^{0}\, \boldsymbol{T}_{t}^{3}\, \boldsymbol{T}_{r}^{t} \boldsymbol{T}_{rh}^{r} \tag{2.78}$$

$$\boldsymbol{T}_{lh}^{0} = \boldsymbol{T}_{3}^{0}\, \boldsymbol{T}_{t}^{3}\, \boldsymbol{T}_{l}^{t} \boldsymbol{T}_{lh}^{l} \tag{2.79}$$

where the matrix $\boldsymbol{T}_{t}^{3}$ describes the transformation imposed by the motion of Joint 4 (dashed line in Fig. 2.28), located at the end-effector of the torso. Frame 4 coincides with Frame t in Fig. 2.27. In view of the property of parameter ϑ_4, it is $\vartheta_4 = -\vartheta_2 - \vartheta_3$, and thus

$$\boldsymbol{T}_{t}^{3} = \begin{bmatrix} c_{23} & s_{23} & 0 & 0 \\ -s_{23} & c_{23} & 0 & 0 \\ 0 & 0 & 1 & 0 \\ 0 & 0 & 0 & 1 \end{bmatrix}.$$

The matrix $\boldsymbol{T}_{3}^{0}$ is given by (2.66), whereas the matrices $\boldsymbol{T}_{r}^{t}$ and $\boldsymbol{T}_{l}^{t}$ relating the torso end-effector frame to the base frames of the two manipulators have constant values. With reference to Fig. 2.28, the elements of these matrices depend on the angle β and on the distances between the origin of Frame t and the origins of Frames r and l. Finally, the expressions of the matrices $\boldsymbol{T}_{rh}^{r}$ and $\boldsymbol{T}_{lh}^{l}$ must be computed by considering the change in the seventh row of the DH parameters table of the DLR manipulator, so as to account for the different kinematic structure of the wrist (see Problem 2.14).

2.10 Joint Space and Operational Space

As described in the previous sections, the direct kinematics equation of a manipulator allows the position and orientation of the end-effector frame to be expressed as a function of the joint variables with respect to the base frame.

If a task is to be specified for the end-effector, it is necessary to assign the end-effector position and orientation, eventually as a function of time (trajectory). This is quite easy for the position. On the other hand, specifying the orientation through the unit vector triplet $(\boldsymbol{n}_e, \boldsymbol{s}_e, \boldsymbol{a}_e)$[11] is quite difficult, since their nine components must be guaranteed to satisfy the orthonormality constraints imposed by (2.4) at each time instant. This problem will be resumed in Chap. 4.

[11] To simplify, the indication of the reference frame in the superscript is omitted.

The problem of describing end-effector orientation admits a natural solution if one of the above minimal representations is adopted. In this case, indeed, a motion trajectory can be assigned to the set of angles chosen to represent orientation.

Therefore, the position can be given by a minimal number of coordinates with regard to the geometry of the structure, and the orientation can be specified in terms of a minimal representation (Euler angles) describing the rotation of the end-effector frame with respect to the base frame. In this way, it is possible to describe the end-effector pose by means of the $(m \times 1)$ vector, with $m \leq n$,

$$\boldsymbol{x}_e = \begin{bmatrix} \boldsymbol{p}_e \\ \boldsymbol{\phi}_e \end{bmatrix} \tag{2.80}$$

where $\boldsymbol{p}_e$ describes the end-effector position and $\boldsymbol{\phi}_e$ its orientation.

This representation of position and orientation allows the description of an end-effector task in terms of a number of inherently independent parameters. The vector $\boldsymbol{x}_e$ is defined in the space in which the manipulator task is specified; hence, this space is typically called *operational space*. On the other hand, the *joint space* (configuration space) denotes the space in which the $(n \times 1)$ vector of joint variables

$$\boldsymbol{q} = \begin{bmatrix} q_1 \\ \vdots \\ q_n \end{bmatrix}, \tag{2.81}$$

is defined; it is $q_i = \vartheta_i$ for a revolute joint and $q_i = d_i$ for a prismatic joint. Accounting for the dependence of position and orientation from the joint variables, the direct kinematics equation can be written in a form other than (2.50), i.e.,

$$\boldsymbol{x}_e = \boldsymbol{k}(\boldsymbol{q}). \tag{2.82}$$

The $(m \times 1)$ vector function $\boldsymbol{k}(\cdot)$ — nonlinear in general — allows computation of the operational space variables from the knowledge of the joint space variables.

It is worth noticing that the dependence of the orientation components of the function $\boldsymbol{k}(\boldsymbol{q})$ in (2.82) on the joint variables is not easy to express except for simple cases. In fact, in the most general case of a six-dimensional operational space ($m = 6$), the computation of the three components of the function $\boldsymbol{\phi}_e(\boldsymbol{q})$ cannot be performed in closed form but goes through the computation of the elements of the rotation matrix, i.e., $\boldsymbol{n}_e(\boldsymbol{q})$, $\boldsymbol{s}_e(\boldsymbol{q})$, $\boldsymbol{a}_e(\boldsymbol{q})$. The equations that allow the determination of the Euler angles from the triplet of unit vectors $\boldsymbol{n}_e$, $\boldsymbol{s}_e$, $\boldsymbol{a}_e$ were given in Sect. 2.4.

Example 2.5

Consider again the three-link planar arm in Fig. 2.20. The geometry of the structure suggests that the end-effector position is determined by the two coordinates p_x and p_y, while its orientation is determined by the angle ϕ formed by the end-effector with the axis x_0. Expressing these operational variables as a function of the joint variables, the two position coordinates are given by the first two elements of the fourth column of the homogeneous transformation matrix (2.63), while the orientation angle is simply given by the sum of joint variables. In sum, the direct kinematics equation can be written in the form

$$\boldsymbol{x}_e = \begin{bmatrix} p_x \\ p_y \\ \phi \end{bmatrix} = \boldsymbol{k}(\boldsymbol{q}) = \begin{bmatrix} a_1 c_1 + a_2 c_{12} + a_3 c_{123} \\ a_1 s_1 + a_2 s_{12} + a_3 s_{123} \\ \vartheta_1 + \vartheta_2 + \vartheta_3 \end{bmatrix}. \tag{2.83}$$

This expression shows that three joint space variables allow specification of at most three independent operational space variables. On the other hand, if orientation is of no concern, it is $\boldsymbol{x}_e = [\, p_x \quad p_y \,]^T$ and there is *kinematic redundancy* of DOFs with respect to a pure positioning end-effector task; this concept will be dealt with in detail afterwards.

2.10.1 Workspace

With reference to the operational space, an index of robot performance is the so-called *workspace*; this is the region described by the origin of the end-effector frame when all the manipulator joints execute all possible motions. It is often customary to distinguish between *reachable* workspace and *dexterous* workspace. The latter is the region that the origin of the end-effector frame can describe while attaining different orientations, while the former is the region that the origin of the end-effector frame can reach with at least one orientation. Obviously, the dexterous workspace is a subspace of the reachable workspace. A manipulator with less than six DOFs cannot take any arbitrary position and orientation in space.

The workspace is characterized by the manipulator geometry and the mechanical joint limits. For an n-DOF manipulator, the reachable workspace is the geometric locus of the points that can be achieved by considering the direct kinematics equation for the sole position part, i.e.,

$$\boldsymbol{p}_e = \boldsymbol{p}_e(\boldsymbol{q}) \qquad q_{im} \leq q_i \leq q_{iM} \quad i = 1, \ldots, n,$$

where q_{im} (q_{iM}) denotes the minimum (maximum) limit at Joint i. This volume is finite, closed, connected — $\boldsymbol{p}_e(\boldsymbol{q})$ is a continuous function — and thus is defined by its bordering surface. Since the joints are revolute or prismatic, it is easy to recognize that this surface is constituted by surface elements of planar, spherical, toroidal and cylindrical type. The manipulator workspace

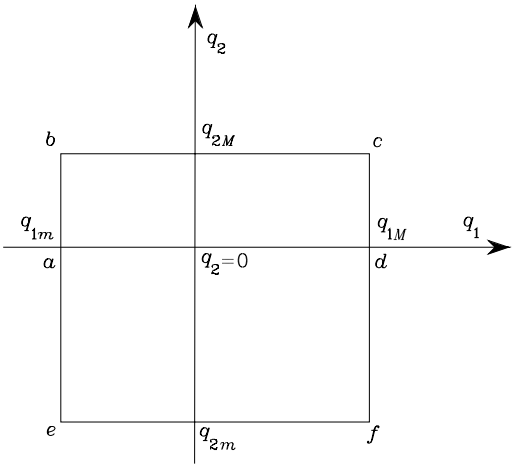

Fig. 2.29. Region of admissible configurations for a two-link arm

(without end-effector) is reported in the data sheet given by the robot manufacturer in terms of a top view and a side view. It represents a basic element to evaluate robot performance for a desired application.

Example 2.6

Consider the simple two-link planar arm. If the mechanical joint limits are known, the arm can attain all the joint space configurations corresponding to the points in the rectangle in Fig. 2.29.

The reachable workspace can be derived via a graphical construction of the image of the rectangle perimeter in the plane of the arm. To this purpose, it is worth considering the images of the segments ab, bc, cd, da, ae, ef, fd. Along the segments ab, bc, cd, ae, ef, fd a loss of mobility occurs due to a joint limit; a loss of mobility occurs also along the segment ad because the arm and forearm are aligned.[12] Further, a change of the arm posture occurs at points a and d: for $q_2 > 0$ the *elbow-down* posture is obtained, while for $q_2 < 0$ the arm is in the *elbow-up* posture.

In the plane of the arm, start drawing the arm in configuration A corresponding to q_{1m} and $q_2 = 0$ (a); then, the segment ab describing motion from $q_2 = 0$ to q_{2M} generates the arc AB; the subsequent arcs BC, CD, DA, AE, EF, FD are generated in a similar way (Fig. 2.30). The external contour of the area $CDAEFHC$ delimits the requested workspace. Further, the area $BCDAB$ is relative to elbow-down postures while the area $DAEFD$ is relative to elbow-up postures; hence, the points in the area $BADHB$ are reachable by the end-effector with both postures.

---

[12] In the following chapter, it will be seen that this configuration characterizes a kinematic *singularity* of the arm.

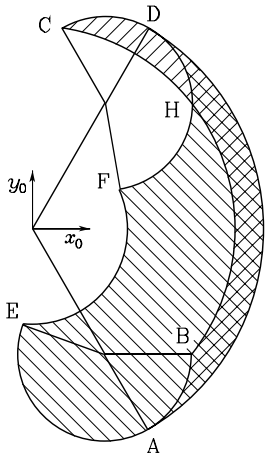

Fig. 2.30. Workspace of a two-link planar arm

In a real manipulator, for a given set of joint variables, the actual values of the operational space variables deviate from those computed via direct kinematics. The direct kinematics equation has indeed a dependence from the DH parameters which is not explicit in (2.82). If the mechanical dimensions of the structure differ from the corresponding parameter of the table because of mechanical tolerances, a deviation arises between the position reached in the assigned posture and the position computed via direct kinematics. Such a deviation is defined *accuracy*; this parameter attains typical values below one millimeter and depends on the structure as well as on manipulator dimensions. Accuracy varies with the end-effector position in the workspace and it is a relevant parameter when robot programming oriented environments are adopted, as will be seen in the last chapter.

Another parameter that is usually listed in the performance data sheet of an industrial robot is *repeatability* which gives a measure of the manipulator's ability to return to a previously reached position; this parameter is relevant for programming an industrial robot by the teaching–by–showing technique which will be presented in Chap. 6. Repeatability depends not only on the characteristics of the mechanical structure but also on the transducers and controller; it is expressed in metric units and is typically smaller than accuracy. For instance, for a manipulator with a maximum reach of 1.5 m, accuracy varies from 0.2 to 1 mm in the workspace, while repeatability varies from 0.02 to 0.2 mm.

2.10.2 Kinematic Redundancy

A manipulator is termed *kinematically redundant* when it has a number of DOFs which is greater than the number of variables that are necessary to

describe a given task. With reference to the above-defined spaces, a manipulator is intrinsically redundant when the dimension of the operational space is smaller than the dimension of the joint space ($m < n$). Redundancy is, anyhow, a concept *relative* to the task assigned to the manipulator; a manipulator can be redundant with respect to a task and nonredundant with respect to another. Even in the case of $m = n$, a manipulator can be functionally redundant when only a number of r components of operational space are of concern for the specific task, with $r < m$.

Consider again the three-DOF planar arm of Sect. 2.9.1. If only the end-effector position (in the plane) is specified, that structure presents a functional redundancy ($n = m = 3$, $r = 2$); this is lost when also the end-effector orientation in the plane is specified ($n = m = r = 3$). On the other hand, a four-DOF planar arm is intrinsically redundant ($n = 4$, $m = 3$).

Yet, take the typical industrial robot with six DOFs; such manipulator is not intrinsically redundant ($n = m = 6$), but it can become functionally redundant with regard to the task to execute. Thus, for instance, in a laser-cutting task a functional redundancy will occur since the end-effector rotation about the approach direction is irrelevant to completion of the task ($r = 5$).

At this point, a question should arise spontaneously: Why to intentionally utilize a redundant manipulator? The answer is to recognize that redundancy can provide the manipulator with dexterity and versatility in its motion. The typical example is constituted by the human arm that has *seven* DOFs: three in the shoulder, one in the elbow and three in the wrist, without considering the DOFs in the fingers. This manipulator is intrinsically redundant; in fact, if the base and the hand position and orientation are both fixed — requiring six DOFs — the elbow can be moved, thanks to the additional available DOF. Then, for instance, it is possible to avoid obstacles in the workspace. Further, if a joint of a redundant manipulator reaches its mechanical limit, there might be other joints that allow execution of the prescribed end-effector motion.

A formal treatment of redundancy will be presented in the following chapter.

2.11 Kinematic Calibration

The Denavit–Hartenberg parameters for direct kinematics need to be computed as precisely as possible in order to improve manipulator accuracy. *Kinematic calibration* techniques are devoted to finding accurate estimates of DH parameters from a series of measurements on the manipulator's end-effector pose. Hence, they do not allow direct measurement of the geometric parameters of the structure.

Consider the direct kinematics equation in (2.82) which can be rewritten by emphasizing the dependence of the operational space variables on the fixed DH parameters, besides the joint variables. Let $\boldsymbol{a} = [\, a_1 \quad \dots \quad a_n \,]^T$, $\boldsymbol{\alpha} =$

$[\alpha_1 \quad \dots \quad \alpha_n]^T$, $\boldsymbol{d} = [d_1 \quad \dots \quad d_n]^T$, and $\boldsymbol{\vartheta} = [\theta_1 \quad \dots \quad \theta_n]^T$ denote the vectors of DH parameters for the whole structure; then (2.82) becomes

$$\boldsymbol{x}_e = \boldsymbol{k}(\boldsymbol{a}, \boldsymbol{\alpha}, \boldsymbol{d}, \boldsymbol{\vartheta}). \tag{2.84}$$

The manipulator's end-effector pose should be measured with high precision for the effectiveness of the kinematic calibration procedure. To this purpose a mechanical apparatus can be used that allows the end-effector to be constrained at given poses with a priori known precision. Alternatively, direct measurement systems of object position and orientation in the Cartesian space can be used which employ triangulation techniques.

Let $\boldsymbol{x}_m$ be the measured pose and $\boldsymbol{x}_n$ the nominal pose that can be computed via (2.84) with the nominal values of the parameters $\boldsymbol{a}$, $\boldsymbol{\alpha}$, $\boldsymbol{d}$, $\boldsymbol{\vartheta}$. The nominal values of the fixed parameters are set equal to the design data of the mechanical structure, whereas the nominal values of the joint variables are set equal to the data provided by the position transducers at the given manipulator posture. The deviation $\Delta\boldsymbol{x} = \boldsymbol{x}_m - \boldsymbol{x}_n$ gives a measure of accuracy at the given posture. On the assumption of small deviations, at first approximation, it is possible to derive the following relation from (2.84):

$$\Delta\boldsymbol{x} = \frac{\partial \boldsymbol{k}}{\partial \boldsymbol{a}}\Delta\boldsymbol{a} + \frac{\partial \boldsymbol{k}}{\partial \boldsymbol{\alpha}}\Delta\boldsymbol{\alpha} + \frac{\partial \boldsymbol{k}}{\partial \boldsymbol{d}}\Delta\boldsymbol{d} + \frac{\partial \boldsymbol{k}}{\partial \boldsymbol{\vartheta}}\Delta\boldsymbol{\vartheta} \tag{2.85}$$

where $\Delta\boldsymbol{a}$, $\Delta\boldsymbol{\alpha}$, $\Delta\boldsymbol{d}$, $\Delta\boldsymbol{\vartheta}$ denote the deviations between the values of the parameters of the real structure and the nominal ones. Moreover, $\partial\boldsymbol{k}/\partial\boldsymbol{a}$, $\partial\boldsymbol{k}/\partial\boldsymbol{\alpha}$, $\partial\boldsymbol{k}/\partial\boldsymbol{d}$, $\partial\boldsymbol{k}/\partial\boldsymbol{\vartheta}$ denote the $(m \times n)$ matrices whose elements are the partial derivatives of the components of the direct kinematics function with respect to the single parameters.[13]

Group the parameters in the $(4n \times 1)$ vector $\boldsymbol{\zeta} = [\boldsymbol{a}^T \quad \boldsymbol{\alpha}^T \quad \boldsymbol{d}^T \quad \boldsymbol{\vartheta}^T]^T$. Let $\Delta\boldsymbol{\zeta} = \boldsymbol{\zeta}_m - \boldsymbol{\zeta}_n$ denote the parameter variations with respect to the nominal values, and $\boldsymbol{\Phi} = [\partial\boldsymbol{k}/\partial\boldsymbol{a} \quad \partial\boldsymbol{k}/\partial\boldsymbol{\alpha} \quad \partial\boldsymbol{k}/\partial\boldsymbol{d} \quad \partial\boldsymbol{k}/\partial\boldsymbol{\vartheta}]$ the $(m \times 4n)$ *kinematic calibration matrix* computed for the nominal values of the parameters $\boldsymbol{\zeta}_n$. Then (2.85) can be compactly rewritten as

$$\Delta\boldsymbol{x} = \boldsymbol{\Phi}(\boldsymbol{\zeta}_n)\Delta\boldsymbol{\zeta}. \tag{2.86}$$

It is desired to compute $\Delta\boldsymbol{\zeta}$ starting from the knowledge of $\boldsymbol{\zeta}_n, \boldsymbol{x}_n$ and the measurement of $\boldsymbol{x}_m$. Since (2.86) constitutes a system of m equations into $4n$ unknowns with $m < 4n$, a sufficient number of end-effector pose measurements has to be performed so as to obtain a system of at least $4n$ equations. Therefore, if measurements are made for a number of l poses, (2.86) yields

$$\Delta\bar{\boldsymbol{x}} = \begin{bmatrix} \Delta\boldsymbol{x}_1 \\ \vdots \\ \Delta\boldsymbol{x}_l \end{bmatrix} = \begin{bmatrix} \boldsymbol{\Phi}_1 \\ \vdots \\ \boldsymbol{\Phi}_l \end{bmatrix} \Delta\boldsymbol{\zeta} = \bar{\boldsymbol{\Phi}}\Delta\boldsymbol{\zeta}. \tag{2.87}$$

[13] These matrices are the Jacobians of the transformations between the parameter space and the operational space.

As regards the nominal values of the parameters needed for the computation of the matrices $\boldsymbol{\Phi}_i$, it should be observed that the geometric parameters are constant whereas the joint variables depend on the manipulator configuration at pose i.

In order to avoid ill-conditioning of matrix $\bar{\boldsymbol{\Phi}}$, it is advisable to choose l so that $lm \gg 4n$ and then solve (2.87) with a least-squares technique; in this case the solution is of the form

$$\Delta\boldsymbol{\zeta} = (\bar{\boldsymbol{\Phi}}^T\bar{\boldsymbol{\Phi}})^{-1}\bar{\boldsymbol{\Phi}}^T\Delta\bar{\boldsymbol{x}} \tag{2.88}$$

where $(\bar{\boldsymbol{\Phi}}^T\bar{\boldsymbol{\Phi}})^{-1}\bar{\boldsymbol{\Phi}}^T$ is the *left pseudo-inverse* matrix of $\bar{\boldsymbol{\Phi}}$.[14] By computing $\bar{\boldsymbol{\Phi}}$ with the nominal values of the parameters $\boldsymbol{\zeta}_n$, the first parameter *estimate* is given by

$$\boldsymbol{\zeta}' = \boldsymbol{\zeta}_n + \Delta\boldsymbol{\zeta}. \tag{2.89}$$

This is a nonlinear parameter estimate problem and, as such, the procedure should be iterated until $\Delta\boldsymbol{\zeta}$ converges within a given threshold. At each iteration, the calibration matrix $\bar{\boldsymbol{\Phi}}$ is to be updated with the parameter estimates $\boldsymbol{\zeta}'$ obtained via (2.89) at the previous iteration. In a similar manner, the deviation $\Delta\bar{\boldsymbol{x}}$ is to be computed as the difference between the measured values for the l end-effector poses and the corresponding poses computed by the direct kinematics function with the values of the parameters at the previous iteration. As a result of the kinematic calibration procedure, more accurate estimates of the real manipulator geometric parameters as well as possible corrections to make on the joint transducers measurements are obtained.

Kinematic calibration is an operation that is performed by the robot manufacturer to guarantee the accuracy reported in the data sheet. There is another kind of calibration that is performed by the robot user which is needed for the measurement system *start-up* to guarantee that the position transducers data are consistent with the attained manipulator posture. For instance, in the case of incremental (nonabsolute) position transducers, such calibration consists of taking the mechanical structure into a given reference posture (*home*) and initializing the position transducers with the values at that posture.

2.12 Inverse Kinematics Problem

The direct kinematics equation, either in the form (2.50) or in the form (2.82), establishes the functional relationship between the joint variables and the end-effector position and orientation. The *inverse kinematics problem* consists of the determination of the joint variables corresponding to a given end-effector position and orientation. The solution to this problem is of fundamental importance in order to transform the motion specifications, assigned to the end-effector in the operational space, into the corresponding joint space motions that allow execution of the desired motion.

[14] See Sect. A.7 for the definition of the pseudo-inverse of a matrix.

As regards the direct kinematics equation in (2.50), the end-effector position and rotation matrix are computed in a unique manner, once the joint variables are known[15]. On the other hand, the inverse kinematics problem is much more complex for the following reasons:

- The equations to solve are in general nonlinear, and thus it is not always possible to find a *closed-form solution*.
- *Multiple solutions* may exist.
- *Infinite solutions* may exist, e.g., in the case of a kinematically redundant manipulator.
- There might be no *admissible* solutions, in view of the manipulator kinematic structure.

The existence of solutions is guaranteed only if the given end-effector position and orientation belong to the manipulator dexterous workspace.

On the other hand, the problem of multiple solutions depends not only on the number of DOFs but also on the number of non-null DH parameters; in general, the greater the number of non-null parameters, the greater the number of admissible solutions. For a six-DOF manipulator without mechanical joint limits, there are in general up to 16 admissible solutions. Such occurrence demands some criterion to choose among admissible solutions (e.g., the elbow-up/elbow-down case of Example 2.6). The existence of mechanical joint limits may eventually reduce the number of admissible multiple solutions for the real structure.

Computation of closed-form solutions requires either *algebraic intuition* to find those significant equations containing the unknowns or *geometric intuition* to find those significant points on the structure with respect to which it is convenient to express position and/or orientation as a function of a reduced number of unknowns. The following examples will point out the ability required to an inverse kinematics problem solver. On the other hand, in all those cases when there are no — or it is difficult to find — closed-form solutions, it might be appropriate to resort to *numerical solution techniques*; these clearly have the advantage of being applicable to any kinematic structure, but in general they do not allow computation of all admissible solutions. In the following chapter, it will be shown how suitable algorithms utilizing the manipulator Jacobian can be employed to solve the inverse kinematics problem.

2.12.1 Solution of Three-link Planar Arm

Consider the arm shown in Fig. 2.20 whose direct kinematics was given in (2.63). It is desired to find the joint variables ϑ_1, ϑ_2, ϑ_3 corresponding to a given end-effector position and orientation.

[15] In general, this cannot be said for (2.82) too, since the Euler angles are not uniquely defined.

As already pointed out, it is convenient to specify position and orientation in terms of a minimal number of parameters: the two coordinates p_x, p_y and the angle ϕ with axis x_0, in this case. Hence, it is possible to refer to the direct kinematics equation in the form (2.83).

A first *algebraic solution* technique is illustrated below. Having specified the orientation, the relation

$$\phi = \vartheta_1 + \vartheta_2 + \vartheta_3 \tag{2.90}$$

is one of the equations of the system to solve[16]. From (2.63) the following equations can be obtained:

$$p_{Wx} = p_x - a_3 c_\phi = a_1 c_1 + a_2 c_{12} \tag{2.91}$$

$$p_{Wy} = p_y - a_3 s_\phi = a_1 s_1 + a_2 s_{12} \tag{2.92}$$

which describe the position of point W, i.e., the origin of Frame 2; this depends only on the first two angles ϑ_1 and ϑ_2. Squaring and summing (2.91), (2.92) yields

$$p_{Wx}^2 + p_{Wy}^2 = a_1^2 + a_2^2 + 2a_1 a_2 c_2$$

from which

$$c_2 = \frac{p_{Wx}^2 + p_{Wy}^2 - a_1^2 - a_2^2}{2a_1 a_2}.$$

The existence of a solution obviously imposes that $-1 \leq c_2 \leq 1$, otherwise the given point would be outside the arm reachable workspace. Then, set

$$s_2 = \pm\sqrt{1 - c_2^2},$$

where the positive sign is relative to the elbow-down posture and the negative sign to the elbow-up posture. Hence, the angle ϑ_2 can be computed as

$$\vartheta_2 = \text{Atan2}(s_2, c_2).$$

Having determined ϑ_2, the angle ϑ_1 can be found as follows. Substituting ϑ_2 into (2.91), (2.92) yields an algebraic system of two equations in the two unknowns s_1 and c_1, whose solution is

$$s_1 = \frac{(a_1 + a_2 c_2) p_{Wy} - a_2 s_2 p_{Wx}}{p_{Wx}^2 + p_{Wy}^2}$$

$$c_1 = \frac{(a_1 + a_2 c_2) p_{Wx} + a_2 s_2 p_{Wy}}{p_{Wx}^2 + p_{Wy}^2}.$$

In analogy to the above, it is

$$\vartheta_1 = \text{Atan2}(s_1, c_1).$$

[16] If ϕ is not specified, then the arm is redundant and there exist infinite solutions to the inverse kinematics problem.

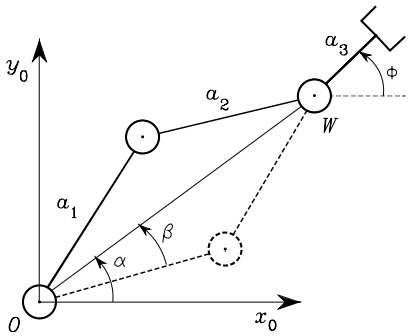

Fig. 2.31. Admissible postures for a two-link planar arm

In the case when $s_2 = 0$, it is obviously $\vartheta_2 = 0, \pi$; as will be shown in the following, in such a posture the manipulator is at a kinematic *singularity*. Yet, the angle ϑ_1 can be determined uniquely, unless $a_1 = a_2$ and it is required $p_{Wx} = p_{Wy} = 0$.

Finally, the angle ϑ_3 is found from (2.90) as

$$\vartheta_3 = \phi - \vartheta_1 - \vartheta_2.$$

An alternative *geometric solution* technique is presented below. As above, the orientation angle is given as in (2.90) and the coordinates of the origin of Frame 2 are computed as in (2.91), (2.92). The application of the cosine theorem to the triangle formed by links a_1, a_2 and the segment connecting points W and O gives

$$p_{Wx}^2 + p_{Wy}^2 = a_1^2 + a_2^2 - 2a_1 a_2 \cos(\pi - \vartheta_2);$$

the two admissible configurations of the triangle are shown in Fig. 2.31. Observing that $\cos(\pi - \vartheta_2) = -\cos\vartheta_2$ leads to

$$c_2 = \frac{p_{Wx}^2 + p_{Wy}^2 - a_1^2 - a_2^2}{2a_1 a_2}.$$

For the existence of the triangle, it must be $\sqrt{p_{Wx}^2 + p_{Wy}^2} \leq a_1 + a_2$. This condition is not satisfied when the given point is outside the arm reachable workspace. Then, under the assumption of admissible solutions, it is

$$\vartheta_2 = \pm\cos^{-1}(c_2);$$

the elbow-up posture is obtained for $\vartheta_2 \in (-\pi, 0)$ while the elbow-down posture is obtained for $\vartheta_2 \in (0, \pi)$.

To find ϑ_1 consider the angles α and β in Fig. 2.31. Notice that the determination of α depends on the sign of p_{Wx} and p_{Wy}; then, it is necessary to compute α as

$$\alpha = \text{Atan2}(p_{Wy}, p_{Wx}).$$

To compute β, applying again the cosine theorem yields

$$c_\beta \sqrt{p_{Wx}^2 + p_{Wy}^2} = a_1 + a_2 c_2$$

and resorting to the expression of c_2 given above leads to

$$\beta = \cos^{-1}\left(\frac{p_{Wx}^2 + p_{Wy}^2 + a_1^2 - a_2^2}{2a_1\sqrt{p_{Wx}^2 + p_{Wy}^2}} \right)$$

with $\beta \in (0, \pi)$ so as to preserve the existence of triangles. Then, it is

$$\vartheta_1 = \alpha \pm \beta,$$

where the positive sign holds for $\vartheta_2 < 0$ and the negative sign for $\vartheta_2 > 0$. Finally, ϑ_3 is computed from (2.90).

It is worth noticing that, in view of the substantial equivalence between the two-link planar arm and the parallelogram arm, the above techniques can be formally applied to solve the inverse kinematics of the arm in Sect. 2.9.2.

2.12.2 Solution of Manipulators with Spherical Wrist

Most of the existing manipulators are kinematically simple, since they are typically formed by an arm, of the kind presented above, and a spherical wrist; see the manipulators in Sects. 2.9.6–2.9.8. This choice is partly motivated by the difficulty to find solutions to the inverse kinematics problem in the general case. In particular, a *six*-DOF kinematic structure has closed-form inverse kinematics solutions if:

- three consecutive revolute joint axes intersect at a common point, like for the spherical wrist;
- three consecutive revolute joint axes are parallel.

In any case, algebraic or geometric intuition is required to obtain closed-form solutions.

Inspired by the previous solution to a three-link planar arm, a suitable point along the structure can be found whose position can be expressed both as a function of the given end-effector position and orientation and as a function of a reduced number of joint variables. This is equivalent to articulating the inverse kinematics problem into two subproblems, since the solution for the *position* is *decoupled* from that for the *orientation*.

For a manipulator with spherical wrist, the natural choice is to locate such point W at the intersection of the three terminal revolute axes (Fig. 2.32). In fact, once the end-effector position and orientation are specified in terms of $\boldsymbol{p}_e$ and $\boldsymbol{R}_e = [\, \boldsymbol{n}_e \quad \boldsymbol{s}_e \quad \boldsymbol{a}_e \,]$, the wrist position can be found as

$$\boldsymbol{p}_W = \boldsymbol{p}_e - d_6 \boldsymbol{a}_e \tag{2.93}$$

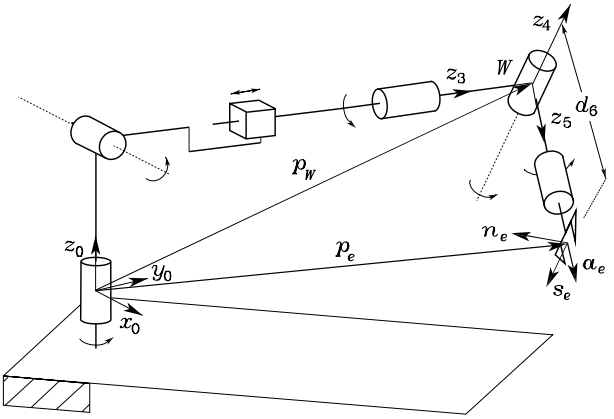

Fig. 2.32. Manipulator with spherical wrist

which is a function of the sole joint variables that determine the arm position[17]. Hence, in the case of a (nonredundant) three-DOF arm, the inverse kinematics can be solved according to the following steps:

- Compute the wrist position $\boldsymbol{p}_W(q_1, q_2, q_3)$ as in (2.93).
- Solve inverse kinematics for (q_1, q_2, q_3).
- Compute $\boldsymbol{R}_3^0(q_1, q_2, q_3)$.
- Compute $\boldsymbol{R}_6^3(\vartheta_4, \vartheta_5, \vartheta_6) = \boldsymbol{R}_3^{0T}\boldsymbol{R}$.
- Solve inverse kinematics for orientation $(\vartheta_4, \vartheta_5, \vartheta_6)$.

Therefore, on the basis of this kinematic decoupling, it is possible to solve the inverse kinematics for the arm separately from the inverse kinematics for the spherical wrist. Below are presented the solutions for two typical arms (spherical and anthropomorphic) as well as the solution for the spherical wrist.

2.12.3 Solution of Spherical Arm

Consider the spherical arm shown in Fig. 2.22, whose direct kinematics was given in (2.65). It is desired to find the joint variables ϑ_1, ϑ_2, d_3 corresponding to a given end-effector position $\boldsymbol{p}_W$.

In order to separate the variables on which $\boldsymbol{p}_W$ depends, it is convenient to express the position of $\boldsymbol{p}_W$ with respect to Frame 1; then, consider the matrix equation

$$(\boldsymbol{A}_1^0)^{-1}\boldsymbol{T}_3^0 = \boldsymbol{A}_2^1\boldsymbol{A}_3^2.$$

[17] Note that the same reasoning was implicitly adopted in Sect. 2.12.1 for the three-link planar arm; $\boldsymbol{p}_W$ described the one-DOF wrist position for the two-DOF arm obtained by considering only the first two links.

Equating the first three elements of the fourth columns of the matrices on both sides yields

$$\boldsymbol{p}_W^1 = \begin{bmatrix} p_{Wx}c_1 + p_{Wy}s_1 \\ -p_{Wz} \\ -p_{Wx}s_1 + p_{Wy}c_1 \end{bmatrix} = \begin{bmatrix} d_3 s_2 \\ -d_3 c_2 \\ d_2 \end{bmatrix} \tag{2.94}$$

which depends only on ϑ_2 and d_3. To solve this equation, set

$$t = \tan \frac{\vartheta_1}{2}$$

so that

$$c_1 = \frac{1 - t^2}{1 + t^2} \qquad s_1 = \frac{2t}{1 + t^2}.$$

Substituting this equation in the third component on the left-hand side of (2.94) gives

$$(d_2 + p_{Wy})t^2 + 2p_{Wx}t + d_2 - p_{Wy} = 0,$$

whose solution is

$$t = \frac{-p_{Wx} \pm \sqrt{p_{Wx}^2 + p_{Wy}^2 - d_2^2}}{d_2 + p_{Wy}}.$$

The two solutions correspond to two different postures. Hence, it is

$$\vartheta_1 = 2\text{Atan2}\left(-p_{Wx} \pm \sqrt{p_{Wx}^2 + p_{Wy}^2 - d_2^2},\ d_2 + p_{Wy}\right).$$

Once ϑ_1 is known, squaring and summing the first two components of (2.94) yields

$$d_3 = \sqrt{(p_{Wx}c_1 + p_{Wy}s_1)^2 + p_{Wz}^2},$$

where only the solution with $d_3 \geq 0$ has been considered. Note that the same value of d_3 corresponds to both solutions for ϑ_1. Finally, if $d_3 \neq 0$, from the first two components of (2.94) it is

$$\frac{p_{Wx}c_1 + p_{Wy}s_1}{-p_{Wz}} = \frac{d_3 s_2}{-d_3 c_2},$$

from which

$$\vartheta_2 = \text{Atan2}(p_{Wx}c_1 + p_{Wy}s_1, p_{Wz}).$$

Notice that, if $d_3 = 0$, then ϑ_2 cannot be uniquely determined.

2.12.4 Solution of Anthropomorphic Arm

Consider the anthropomorphic arm shown in Fig. 2.23. It is desired to find the joint variables ϑ_1, ϑ_2, ϑ_3 corresponding to a given end-effector position $\boldsymbol{p}_W$. Notice that the direct kinematics for $\boldsymbol{p}_W$ is expressed by (2.66) which can

be obtained from (2.70) by setting $d_6 = 0$, $d_4 = a_3$ and replacing ϑ_3 with the angle $\vartheta_3 + \pi/2$ because of the misalignment of the Frames 3 for the structures in Fig. 2.23 and in Fig. 2.26, respectively. Hence, it follows

$$p_{Wx} = c_1(a_2c_2 + a_3c_{23}) \tag{2.95}$$
$$p_{Wy} = s_1(a_2c_2 + a_3c_{23}) \tag{2.96}$$
$$p_{Wz} = a_2s_2 + a_3s_{23}. \tag{2.97}$$

Proceeding as in the case of the two-link planar arm, it is worth squaring and summing (2.95)–(2.97) yielding

$$p_{Wx}^2 + p_{Wy}^2 + p_{Wz}^2 = a_2^2 + a_3^2 + 2a_2a_3c_3$$

from which

$$c_3 = \frac{p_{Wx}^2 + p_{Wy}^2 + p_{Wz}^2 - a_2^2 - a_3^2}{2a_2a_3} \tag{2.98}$$

where the admissibility of the solution obviously requires that $-1 \leq c_3 \leq 1$, or equivalently $|a_2 - a_3| \leq \sqrt{p_{Wx}^2 + p_{Wy}^2 + p_{Wz}^2} \leq a_2 + a_3$, otherwise the wrist point is outside the reachable workspace of the manipulator. Hence it is

$$s_3 = \pm\sqrt{1 - c_3^2} \tag{2.99}$$

and thus

$$\vartheta_3 = \text{Atan2}(s_3, c_3)$$

giving the two solutions, according to the sign of s_3,

$$\vartheta_{3,\text{I}} \in [-\pi, \pi] \tag{2.100}$$
$$\vartheta_{3,\text{II}} = -\vartheta_{3,I}. \tag{2.101}$$

Having determined ϑ_3, it is possible to compute ϑ_2 as follows. Squaring and summing (2.95), (2.96) gives

$$p_{Wx}^2 + p_{Wy}^2 = (a_2c_2 + a_3c_{23})^2$$

from which

$$a_2c_2 + a_3c_{23} = \pm\sqrt{p_{Wx}^2 + p_{Wy}^2}. \tag{2.102}$$

The system of the two Eqs. (2.102), (2.97), for each of the solutions (2.100), (2.101), admits the solutions:

$$c_2 = \frac{\pm\sqrt{p_{Wx}^2 + p_{Wy}^2}(a_2 + a_3c_3) + p_{Wz}a_3s_3}{a_2^2 + a_3^2 + 2a_2a_3c_3} \tag{2.103}$$

$$s_2 = \frac{p_{Wz}(a_2 + a_3c_3) \mp \sqrt{p_{Wx}^2 + p_{Wy}^2}a_3s_3}{a_2^2 + a_3^2 + 2a_2a_3c_3}. \tag{2.104}$$

From (2.103), (2.104) it follows

$$\vartheta_2 = \text{Atan2}(s_2, c_2)$$

which gives the four solutions for ϑ_2, according to the sign of s_3 in (2.99):

$$\vartheta_{2,\text{I}} = \text{Atan2}\left((a_2 + a_3 c_3)p_{Wz} - a_3 s_3^+ \sqrt{p_{Wx}^2 + p_{Wy}^2},\right.$$
$$\left.(a_2 + a_3 c_3)\sqrt{p_{Wx}^2 + p_{Wy}^2} + a_3 s_3^+ p_{Wz}\right) \tag{2.105}$$

$$\vartheta_{2,\text{II}} = \text{Atan2}\left((a_2 + a_3 c_3)p_{Wz} + a_3 s_3^+ \sqrt{p_{Wx}^2 + p_{Wy}^2},\right.$$
$$\left.-(a_2 + a_3 c_3)\sqrt{p_{Wx}^2 + p_{Wy}^2} + a_3 s_3^+ p_{Wz}\right) \tag{2.106}$$

corresponding to $s_3^+ = \sqrt{1 - c_3^2}$, and

$$\vartheta_{2,\text{III}} = \text{Atan2}\left((a_2 + a_3 c_3)p_{Wz} - a_3 s_3^- \sqrt{p_{Wx}^2 + p_{Wy}^2},\right.$$
$$\left.(a_2 + a_3 c_3)\sqrt{p_{Wx}^2 + p_{Wy}^2} + a_3 s_3^- p_{Wz}\right) \tag{2.107}$$

$$\vartheta_{2,\text{IV}} = \text{Atan2}\left((a_2 + a_3 c_3)p_{Wz} + a_3 s_3^- \sqrt{p_{Wx}^2 + p_{Wy}^2},\right.$$
$$\left.-(a_2 + a_3 c_3)\sqrt{p_{Wx}^2 + p_{Wy}^2} + a_3 s_3^- p_{Wz}\right) \tag{2.108}$$

corresponding to $s_3^- = -\sqrt{1 - c_3^2}$.

Finally, to compute ϑ_1, it is sufficient to rewrite (2.95), (2.96), using (2.102), as

$$p_{Wx} = \pm c_1 \sqrt{p_{Wx}^2 + p_{Wy}^2}$$
$$p_{Wy} = \pm s_1 \sqrt{p_{Wx}^2 + p_{Wy}^2}$$

which, once solved, gives the two solutions:

$$\vartheta_{1,\text{I}} = \text{Atan2}(p_{Wy}, p_{Wx}) \tag{2.109}$$
$$\vartheta_{1,\text{II}} = \text{Atan2}(-p_{Wy}, -p_{Wx}). \tag{2.110}$$

Notice that (2.110) gives[18]

$$\vartheta_{1,\text{II}} = \begin{cases} \text{Atan2}(p_{Wy}, p_{Wx}) - \pi & p_{Wy} \geq 0 \\ \text{Atan2}(p_{Wy}, p_{Wx}) + \pi & p_{Wy} < 0. \end{cases}$$

[18] It is easy to show that $\text{Atan2}(-y, -x) = -\text{Atan2}(y, -x)$ and

$$\text{Atan2}(y, -x) = \begin{cases} \pi - \text{Atan2}(y, x) & y \geq 0 \\ -\pi - \text{Atan2}(y, x) & y < 0. \end{cases}$$

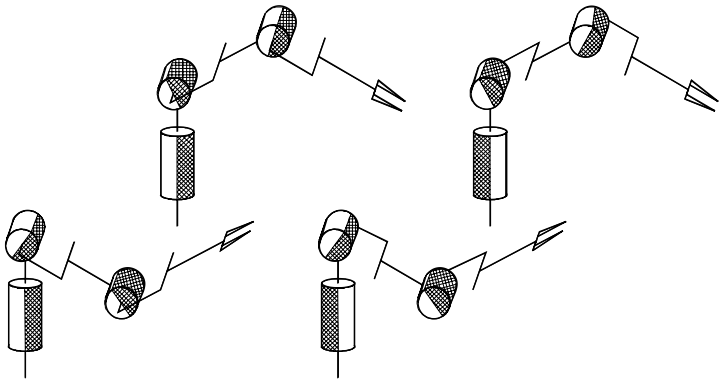

Fig. 2.33. The four configurations of an anthropomorphic arm compatible with a given wrist position

As can be recognized, there exist four solutions according to the values of ϑ_3 in (2.100), (2.101), ϑ_2 in (2.105)–(2.108) and ϑ_1 in (2.109), (2.110):

$$(\vartheta_{1,\mathrm{I}}, \vartheta_{2,\mathrm{I}}, \vartheta_{3,\mathrm{I}}) \quad (\vartheta_{1,\mathrm{I}}, \vartheta_{2,\mathrm{III}}, \vartheta_{3,\mathrm{II}}) \quad (\vartheta_{1,\mathrm{II}}, \vartheta_{2,\mathrm{II}}, \vartheta_{3,\mathrm{I}}) \quad (\vartheta_{1,\mathrm{II}}, \vartheta_{2,\mathrm{IV}}, \vartheta_{3,\mathrm{II}}),$$

which are illustrated in Fig. 2.33: shoulder–right/elbow–up, shoulder–left/elbow–up, shoulder–right/elbow–down, shoulder–left/elbow–down; obviously, the forearm orientation is different for the two pairs of solutions.

Notice finally how it is possible to find the solutions only if at least

$$p_{Wx} \neq 0 \qquad \text{or} \qquad p_{Wy} \neq 0.$$

In the case $p_{Wx} = p_{Wy} = 0$, an infinity of solutions is obtained, since it is possible to determine the joint variables ϑ_2 and ϑ_3 independently of the value of ϑ_1; in the following, it will be seen that the arm in such configuration is kinematically *singular* (see Problem 2.18).

2.12.5 Solution of Spherical Wrist

Consider the spherical wrist shown in Fig. 2.24, whose direct kinematics was given in (2.67). It is desired to find the joint variables ϑ_4, ϑ_5, ϑ_6 corresponding to a given end-effector orientation $\boldsymbol{R}_6^3$. As previously pointed out, these angles constitute a set of Euler angles ZYZ with respect to Frame 3. Hence, having computed the rotation matrix

$$\boldsymbol{R}_6^3 = \begin{bmatrix} n_x^3 & s_x^3 & a_x^3 \\ n_y^3 & s_y^3 & a_y^3 \\ n_z^3 & s_z^3 & a_z^3 \end{bmatrix},$$

from its expression in terms of the joint variables in (2.67), it is possible to compute the solutions directly as in (2.19), (2.20), i.e.,

$$\begin{aligned} \vartheta_4 &= \text{Atan2}(a_y^3, a_x^3) \\ \vartheta_5 &= \text{Atan2}\Big(\sqrt{(a_x^3)^2 + (a_y^3)^2}, a_z^3\Big) \\ \vartheta_6 &= \text{Atan2}(s_z^3, -n_z^3) \end{aligned} \tag{2.111}$$

for $\vartheta_5 \in (0, \pi)$, and

$$\begin{aligned} \vartheta_4 &= \text{Atan2}(-a_y^3, -a_x^3) \\ \vartheta_5 &= \text{Atan2}\Big(-\sqrt{(a_x^3)^2 + (a_y^3)^2}, a_z^3\Big) \\ \vartheta_6 &= \text{Atan2}(-s_z^3, n_z^3) \end{aligned} \tag{2.112}$$

for $\vartheta_5 \in (-\pi, 0)$.

Bibliography

The treatment of kinematics of robot manipulators can be found in several classical robotics texts, such as [180, 10, 200, 217]. Specific texts are [23, 6, 151].

For the descriptions of the orientation of a rigid body, see [187]. Quaternion algebra can be found in [46]; see [204] for the extraction of quaternions from rotation matrices.

The Denavit–Hartenberg convention was first introduced in [60]. A modified version is utilized in [53, 248, 111]. The use of homogeneous transformation matrices for the computation of open-chain manipulator direct kinematics is presented in [181], while in [183] sufficient conditions are given for the closed-form computation of the inverse kinematics problem. For kinematics of closed chains see [144, 111]. The design of the Stanford manipulator is due to [196].

The problem of kinematic calibration is considered in [188, 98]. Methods which do not require the use of external sensors for direct measurement of end-effector position and orientation are proposed in [68].

The kinematic decoupling deriving from the spherical wrist is utilized in [76, 99, 182]. Numerical methods for the solution of the inverse kinematics problem based on iterative algorithms are proposed in [232, 86].

Problems

2.1. Find the rotation matrix corresponding to the set of Euler angles ZXZ.

2.2. Discuss the inverse solution for the Euler angles ZYZ in the case $s_\vartheta = 0$.

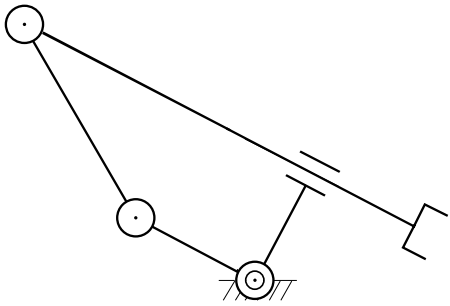

Fig. 2.34. Four-link closed-chain planar arm with prismatic joint

2.3. Discuss the inverse solution for the Roll–Pitch–Yaw angles in the case $c_\vartheta = 0$.

2.4. Verify that the rotation matrix corresponding to the rotation by an angle about an arbitrary axis is given by (2.25).

2.5. Prove that the angle and the unit vector of the axis corresponding to a rotation matrix are given by (2.27), (2.28). Find inverse formulae in the case of $\sin\vartheta = 0$.

2.6. Verify that the rotation matrix corresponding to the unit quaternion is given by (2.33).

2.7. Prove that the unit quaternion is invariant with respect to the rotation matrix and its transpose, i.e., $\boldsymbol{R}(\eta, \boldsymbol{\epsilon})\boldsymbol{\epsilon} = \boldsymbol{R}^T(\eta, \boldsymbol{\epsilon})\boldsymbol{\epsilon} = \boldsymbol{\epsilon}$.

2.8. Prove that the unit quaternion corresponding to a rotation matrix is given by (2.34), (2.35).

2.9. Prove that the quaternion product is expressed by (2.37).

2.10. By applying the rules for inverting a block-partitioned matrix, prove that matrix $\boldsymbol{A}_0^1$ is given by (2.45).

2.11. Find the direct kinematics equation of the four-link closed-chain planar arm in Fig. 2.34, where the two links connected by the prismatic joint are orthogonal to each other

2.12. Find the direct kinematics equation for the cylindrical arm in Fig. 2.35.

2.13. Find the direct kinematics equation for the SCARA manipulator in Fig. 2.36.

2.14. Find the complete direct kinematics equation for the humanoid manipulator in Fig. 2.28.

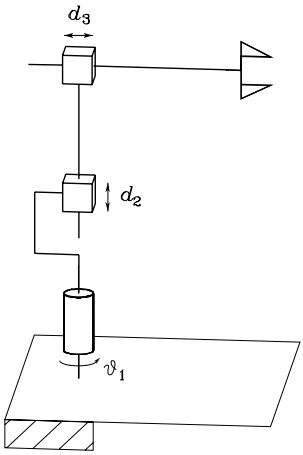

Fig. 2.35. Cylindrical arm

2.15. For the set of minimal representations of orientation $\boldsymbol{\phi}$, define the sum operation in terms of the composition of rotations. By means of an example, show that the commutative property does not hold for that operation.

2.16. Consider the elementary rotations about coordinate axes given by infinitesimal angles. Show that the rotation resulting from any two elementary rotations does not depend on the order of rotations. [*Hint*: for an infinitesimal angle $d\phi$, approximate $\cos(d\phi) \approx 1$ and $\sin(d\phi) \approx d\phi \ldots$]. Further, define $\boldsymbol{R}(d\phi_x, d\phi_y, d\phi_z) = \boldsymbol{R}_x(d\phi_x)\boldsymbol{R}_y(d\phi_y)\boldsymbol{R}_z(d\phi_z)$; show that

$$\boldsymbol{R}(d\phi_x, d\phi_y, d\phi_z)\boldsymbol{R}(d\phi'_x, d\phi'_y, d\phi'_z) = \boldsymbol{R}(d\phi_x + d\phi'_x, d\phi_y + d\phi'_y, d\phi_z + d\phi'_z).$$

2.17. Draw the workspace of the three-link planar arm in Fig. 2.20 with the data:

$$a_1 = 0.5 \qquad a_2 = 0.3 \qquad a_3 = 0.2$$

$$-\pi/3 \leq q_1 \leq \pi/3 \qquad -2\pi/3 \leq q_2 \leq 2\pi/3 \qquad -\pi/2 \leq q_3 \leq \pi/2.$$

2.18. With reference to the inverse kinematics of the anthropomorphic arm in Sect. 2.12.4, discuss the number of solutions in the singular cases of $s_3 = 0$ and $p_{Wx} = p_{Wy} = 0$.

2.19. Solve the inverse kinematics for the cylindrical arm in Fig. 2.35.

2.20. Solve the inverse kinematics for the SCARA manipulator in Fig. 2.36.

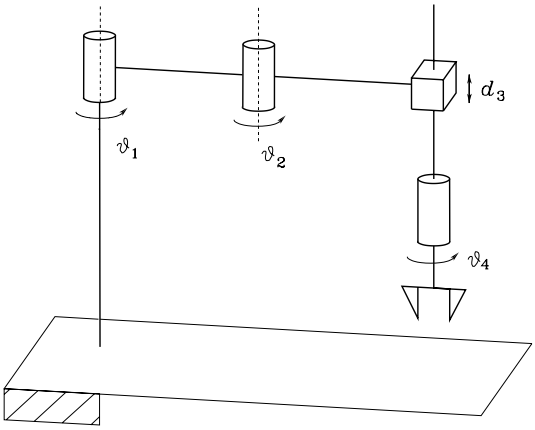

Fig. 2.36. SCARA manipulator